

# Tribological Properties Research of Texturally Modified Titanium Alloy Materials

Fan Qu<sup>1</sup>, Xinhao Yang<sup>1</sup>, Wen Zhong<sup>1\*</sup>, Yongxian Chen<sup>2</sup>,

<sup>1</sup> School of Mechanical Engineering, Xihua University

#9999, Hongguang Avenue, Pidu District, Chengdu, China, 610039

1281049378@qq.com; 18080028693@163.com; zw1019@126.com

<sup>2</sup> Chengdu Special Equipment Inspection and Testing Research Institute

#255, Wulian 1st Road, Shuangliu District, Chengdu, China, 610200

mnb414109@163.com

**Abstract** -The application of titanium alloys in frictional environments is significantly hindered by their inherent drawbacks, such as high friction coefficients, elevated wear rates, and poor wear resistance. To address these issues, this study employs laser engraving to texture the surface of titanium alloys. The tribological properties of the treated surfaces are characterized using spectral confocal two-dimensional profilometry, ultra-depth three-dimensional microscopy, and electron microscopy. The results are as follows:

1.Surface texturing demonstrates a measurable improvement in the tribological performance of titanium alloys, with the extent of improvement contingent upon the shape of the texture pattern. Specifically, the friction coefficient of the pitcher plant-inspired texture decreased by 24.5%, while the shark skin-inspired texture exhibited an 18.4% reduction. Comprehensive analysis of friction coefficients and wear rates indicates that the pitcher plant-inspired texture yields the most significant enhancement in tribological performance, whereas the shark skin-inspired texture shows the least improvement.

2.The effectiveness of bio-inspired textures in improving the tribological properties of titanium alloys varies with their lateral dimensions and density. As the lateral dimensions of the textures increase, their ability to reduce friction and enhance wear resistance diminishes. Similarly, a decrease in texture density results in a reduction in their beneficial effects.

This study represents the first systematic investigation into the impact of four bio-inspired textures, including pitcher plant and shark skin patterns, on the tribological performance of TC4 titanium alloy. Furthermore, through parameter optimization, critical thresholds for texture dimensions and density are identified, providing valuable insights for future applications.

**Keywords:** TC4 titanium alloy; Surface modification; Biomimetic micro-texture; Tribological properties; Texture parameter optimization

© Copyright 2025 Authors - This is an Open Access article published under the Creative Commons Attribution License terms (<http://creativecommons.org/licenses/by/3.0>). Unrestricted use, distribution, and reproduction in any medium are permitted, provided the original work is properly cited.

## 1. Introduction

Titanium alloy, renowned for its exceptional properties such as high strength, low density, and excellent corrosion resistance, has found extensive applications in industries including aerospace, automotive manufacturing, and medical devices. However, its utility in frictional environments is significantly limited by inherent drawbacks such as excessive surface friction coefficients, high wear rates, and inadequate wear resistance. To enhance the wear resistance of titanium alloys, it is imperative to adopt appropriate processing techniques aimed at improving their tribological performance[1].

With advancements in micro- and nano-fabrication technologies and the deepening exploration of tribological theories, an increasing body of experimental evidence suggests that surfaces with controlled roughness or intricate textures can exhibit superior tribological properties. By texturing material surfaces, the interaction between friction pairs can be effectively optimized, leading to enhanced lubrication performance and significantly improved wear resistance[2].

Hamilton et al.[3] pioneered the use of etching technology to create micron-level protrusions on the surface of seals. Through both theoretical and experimental investigations, they demonstrated that these micro-scale protrusions could generate hydrodynamic lubrication effects, effectively reducing the friction coefficient. Over the past few decades, surface texturing has achieved significant progress in enhancing the wear resistance of cutting tools[4] and improving the anti-wear performance of gear pump friction pairs[5], among other applications.

The advancement of bionics has provided new principles, ideas, and theories for scientific progress and technological innovation[6], leading to the application of bionics in surface texturing. Sun et al.[7] conducted an in-depth study on the unique crescent-shaped microstructure of pitcher plants, revealing its low surface adhesion, reduced friction, and even self-cleaning properties. Cui et al.[8] analyzed the epidermal structures of dung beetles and hammerhead sharks and, inspired by their functional characteristics and geometric shapes, utilized laser surface texturing technology to create corresponding biomimetic microstructures on ceramic cutting tools. Intermittent turning experiments demonstrated that tools with biomimetic surfaces exhibited superior cutting performance and significantly enhanced wear resistance. Zhang et al.[9] designed a riblet microstructure inspired by the valve structure of

shells and fabricated these riblets at specific intervals on the surfaces of test samples. Wear tests showed that, compared to flat samples, the wear of 65Mn and T10 samples with riblets was reduced by 17% to 30% and 13% to 24%, respectively. Du et al.[10] designed a rectangular microstructure based on the texture of pangolin scales and integrated this microstructure into cutting tools. A series of simulation analyses revealed that this design significantly reduced cutting forces and tool temperature rise during machining, thereby demonstrating excellent wear resistance.

Despite the remarkable anti-wear performance demonstrated by biomimetic textures in ceramic and steel-based materials, their application in titanium alloys remains significantly underexplored, particularly with respect to the quantitative relationship between texture parameters (size, density) and tribological performance. In this study, laser engraving technology was employed to fabricate four types of biomimetic textures on the surface of TC4 titanium alloy, systematically investigating their effects on the frictional properties of the material.

**2. Test section**

**2.1 Test materials and equipment**

The primary materials utilized in this study include titanium alloy, calcium-based bentonite, and ammonium molybdate, as detailed in Table 1. The experimental instruments and equipment employed are listed in Table 2.

Table.1 Main raw materials

Name	Specification	Manufacturer
Calcium-based bentonite	400 mesh	Zongrun Mineral Products Co., Ltd.
Ammonium molybdate	High purity	Chengdu Kelong Chemical Co., Ltd.
Thiourea	Analytical grade	Chengdu Kelong Chemical Co., Ltd.
Silicon nitride ceramic ball	6 mm	Yuncheng Yaste Steel Ball Co., Ltd.
Titanium alloy	TC4	Xinyi Metal Materials Co., Ltd.

Table.2 Test instruments and equipments

Name	Model/Specification	Manufacturer
Reciprocating friction and wear tester	MWF-02	Sichuan Jiaoyang Technology Co., Ltd.
Mechanical ultrasonic cleaner	KX	Beijing Kexi Century Technology Co., Ltd.
Laboratory ultrapure water system	XUC-10L	Shanghai Xiniu Lab Instrument Co., Ltd.

Electronic balance	FA2004	Shanghai Sunny Hengping Scientific Instrument Co., Ltd.
Automatic single-disc grinding and polishing machine	CV-MP-3Q	Sivaka Precision Instruments (Dongguan) Co., Ltd.
Laser marking machine	Desktop type	Shandong Tianyou Laser Equipment Co., Ltd.
High-pressure reactor	KH	Shanghai Lichen Bangxi Instrument Technology Co., Ltd.
Spectral confocal 2D profilometer	SM-5000	Sixian Photoelectric Technology (Shanghai) Co., Ltd.
Ultra-depth 3D display system	VS-TA2	Huanxian Technology (Shanghai) Co., Ltd.
High-temperature drying oven	SN-GWX-150B	Shanghai Shangpu Instrument Equipment Co., Ltd.

## 2.2 Preparation of 0.25%wt MoS<sub>2</sub>Bentonite Aqueous Solution

A total of 120 mg of ammonium molybdate and 210 mg of thiourea were added to 30 mL of distilled water, followed by magnetic stirring at room temperature for 15 minutes to form a homogeneous suspension. The suspension was then transferred into a 50 mL stainless steel autoclave lined with polytetrafluoroethylene (PTFE). After sealing, the autoclave was maintained at 200°C for 24 hours. Upon completion of the reaction, the system was cooled to room temperature, and the black precipitate was collected via vacuum filtration. The precipitate was washed three times with ethanol to remove impurities. The resulting product was dried in a vacuum oven at 70°C for 24 hours to obtain MoS<sub>2</sub> powder.

Next, 100 mL of ultrapure water was placed in a beaker, and 0.25 g of MoS<sub>2</sub> powder and 4.75 g of calcium-based bentonite (400 mesh) were sequentially added to the ultrapure water. The mixture was stirred with a glass rod and then transferred to a mechanical ultrasonic cleaner, where it was ultrasonically dispersed at a

frequency of 40 kHz for 10 minutes. This process yielded the final 0.25%wt MoS<sub>2</sub> bentonite aqueous solution.

## 2.3 Design and Fabrication of Biomimetic Textures

Research has shown that regularly arranged micro-dimpled structures can significantly reduce the friction coefficient, wear volume, and wear rate of friction materials, with their performance influenced by the shape, size, density, and pattern of the dimples[11, 12]. Common dimple morphologies include squares, hexagons, rectangles, circles, and parallel or grid-like grooves. However, literature analysis indicates that the improvement in tribological performance achieved by geometric textures is far inferior to that of biomimetic textures.

Based on the functional similarity principle of bionics, this study optimized the crescent-shaped microstructure of the wax zone in pitcher plants, the papillary microtexture of banana leaf surfaces, the microstructures of shark skin, and the ribbed structures on the surfaces of scallop valves. These optimizations led to the design of four biomimetic texture morphologies: Nepenthes, Banana leaf, Shark skin, and Scallop, as illustrated in Figure 1.



Figure.1 Four biomimetic micro-texture shapes

Currently, the fabrication of surface textures has reached a high level of sophistication, with a variety of advanced techniques available, including laser

processing[13], precision cutting technology[14], and micro-abrasive jet machining[15].

In this study, laser processing technology was employed to create textured patterns on the surface of

TC4 titanium alloy. Prior to processing, the samples were sequentially ground using 60#, 150#, 240#, 400#, 600#, and 1200# sandpaper, followed by ultrasonic cleaning in anhydrous ethanol for 20 minutes[16]. The laser engraving parameters were uniformly set as follows: engraving count of 1 pass, processing speed of 100 mm/s, frequency of 30 kHz, pulse width of 1  $\mu$ s, current of 1 A, open delay of 300  $\mu$ s, close delay of 150  $\mu$ s, end delay of 300  $\mu$ s, and corner delay of 100  $\mu$ s. To investigate the influence of different texture patterns on the tribological performance of TC4 titanium alloy, the

dimensions of all textures in the experiment were fixed at 250  $\mu$ m, with both horizontal and vertical spacings set at 50  $\mu$ m (see Table 3). After identifying the optimal texture pattern, key parameters for enhancing anti-friction and wear resistance, including texture size and area ratio, were further optimized. Specifically, textures with horizontal dimensions of 250  $\mu$ m, 400  $\mu$ m, and 550  $\mu$ m were fabricated (see Table 4), along with textures of varying densities characterized by horizontal spacings of 50  $\mu$ m, 100  $\mu$ m, and 150  $\mu$ m, and vertical spacings of 50  $\mu$ m, 100  $\mu$ m, and 150  $\mu$ m (see Table 5).

Table.3 Geometric parameters of different textures

Bionic texture shape	Diameter ( $\mu$ m)	Area rate
Nepenthes	250	80%
Banana leaf	250	80%
Shark skin	250	80%
Scallop	250	80%

Table.4 Geometric parameters of different diameters

Bionic texture shape	Diameter ( $\mu$ m)	Area rate
Nepenthes	250	80%
Nepenthes	400	80%
Nepenthes	550	80%

Table.5 Geometric parameters of different densities

Bionic texture shape	Diameter ( $\mu$ m)	Area rate
Nepenthes	250	60%
Nepenthes	250	70%
Nepenthes	250	80%

Figure 2 below shows the ultra-depth 3D system display of biomimetic textures engraved on the surface of TC4 titanium alloy using a laser engraving machine.

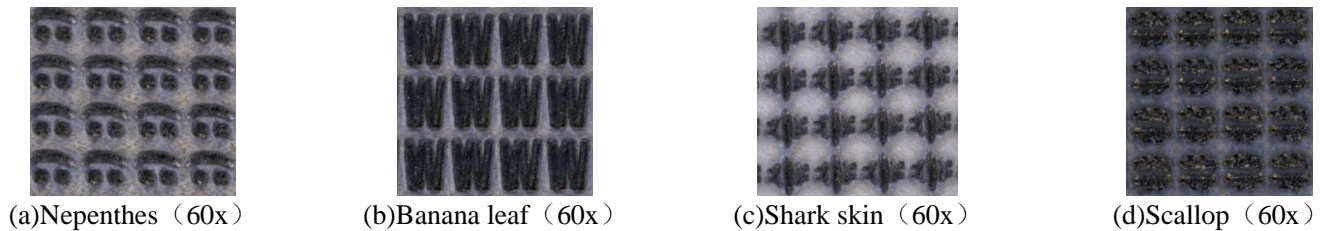


Figure.2 Four kinds of texture surface morphologies captured by the ultra-depth of field 3D display system

## 2.4 Friction Testing

The friction tests were conducted using a ball-on-disk reciprocating friction and wear tester (MWF-02) with a reciprocating sliding distance of 8 mm. A friction pair consisting of a silicon nitride ceramic ball and the

sample was employed. The testing parameters were set as follows: frequency of 2 Hz, load of 20 N, duration of 0.5 hours, and ambient temperature. The tests were performed under lubrication with a 0.25%wt MoS<sub>2</sub> bentonite aqueous solution. A schematic diagram of the friction pair is illustrated in Figure 3.

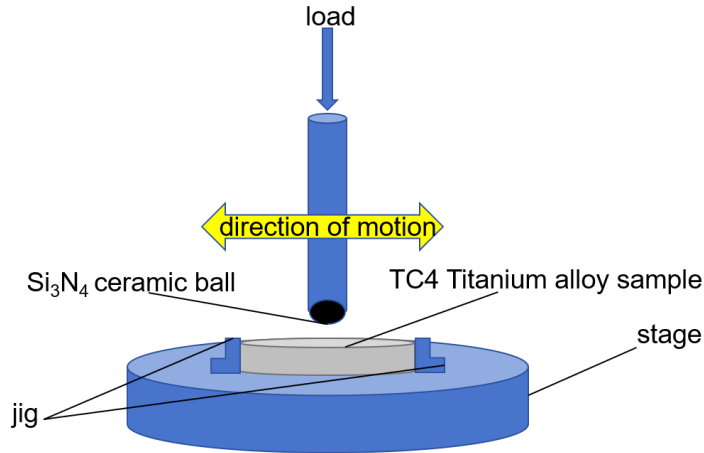


Figure.3 Friction pair diagram

### 3. Results and Discussion

#### 3.1 Influence of different weaving schemes on tribological properties of TC4 titanium alloy (1) Analysis of Friction Coefficient Variation

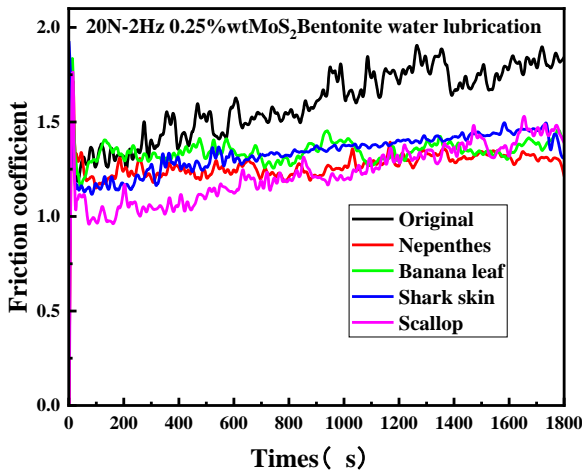


Figure.4 Comparison of friction coefficient between TC4 titanium alloy sample with different surface texture and original plate

From the analysis of Figure 4, it can be observed that the friction coefficient of the TC4 titanium alloy samples changes correspondingly when the surface texture is altered. A comparison reveals that the friction coefficients of all four textured samples are lower than that of the original sample. This indicates that the TC4 titanium alloy samples with biomimetic textures exhibit superior tribological performance compared to the original sample. The surface texturing significantly

enhances the anti-friction properties of the titanium alloy material. Biomimetic textures with different patterns were engraved on the surface of TC4 titanium alloy samples. For comparison, a sample without any texture (referred to as the original sample) was also included. The variation in the friction coefficient of the TC4 titanium alloy samples at room temperature was observed and analyzed.

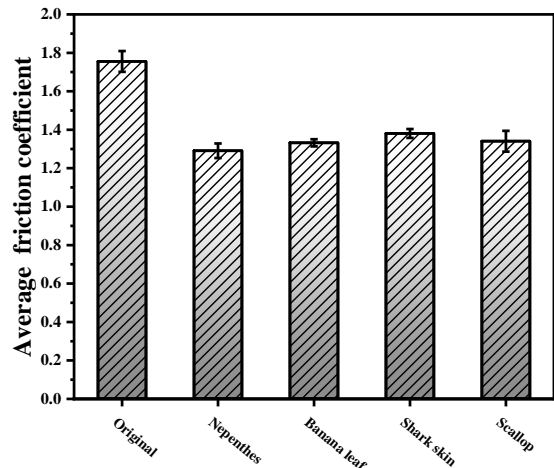


Figure.5 Comparison of average friction coefficient between TC4 titanium alloy sample with different surface texture and original plate

enhances the anti-friction properties of the titanium alloy material.

By calculating the average friction coefficient during the stable friction phase after 600 seconds, the following results were obtained: the original sample had an average friction coefficient of 1.701, pitcher plant texture of 1.285, banana leaf texture of 1.349, shark skin texture of 1.387, and scallop texture of 1.303. Further calculations revealed that the pitcher plant texture

exhibited the greatest reduction in friction coefficient compared to the original sample, at 24.5%, followed by the scallop texture at 23.4%, the banana leaf texture at 20.7%, and the shark skin texture with the least reduction at 18.5%. Over time, as the system stabilized, the friction coefficient of the pitcher plant texture remained lower than those of the other three textures. This demonstrates that the pitcher plant texture provides the best improvement in anti-friction performance for the TC4 titanium alloy surface, followed by the scallop texture, the banana leaf texture, and finally

the shark skin texture, which performed the least effectively.

### (2) Analysis of Wear Rate Variation

Figure 10 illustrates the wear rates of different texture patterns at room temperature. The height of the cylindrical bars in the figure indicates that the wear rates of the textured TC4 titanium alloy samples are all lower than that of the original sample. This demonstrates that surface biomimetic texturing enhances the wear resistance of titanium alloy materials.

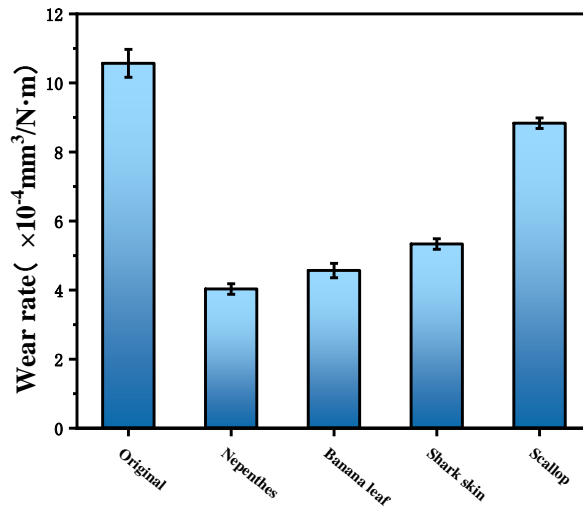


Figure.6 Comparison of the wear rate of TC4 titanium alloy with the original sheet in different weaving cases

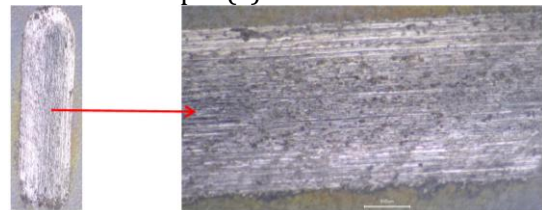
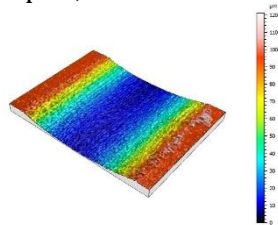
By calculating the reduction in wear rates, it was found that the pitcher plant texture exhibited a 44.6% decrease, the banana leaf texture a 61.7% decrease, the shark skin texture a 55.4% decrease, and the scallop texture a 28.1% decrease. These results indicate that the banana leaf texture provides the most significant improvement in the wear resistance of the titanium alloy surface, followed by the shark skin texture, the pitcher plant texture, and finally the scallop texture, which performed the least effectively.

### (3) Surface Morphology Analysis

Figure 7 presents the three-dimensional and cross-sectional two-dimensional wear scar profiles of TC4 titanium alloy samples, both untreated and engraved

with the four textures. From the figure, it is evident that Figure 7(a), representing the original sample, exhibits a wide and deep wear track, with a wear scar depth and width of 90  $\mu\text{m}$  and 1.6 mm, respectively. This indicates that the titanium alloy material, without any surface treatment, demonstrates poor anti-friction and wear resistance properties.

In contrast, the wear scars of the textured samples—Figure 7(b) pitcher plant, (c) banana leaf, (d) shark skin, and (e) scallop—show reduced depths compared to (a). The wear scar depths and widths are 69  $\mu\text{m}$  and 1.4 mm, 79  $\mu\text{m}$  and 1.3 mm, 73  $\mu\text{m}$  and 1.2 mm, and 89  $\mu\text{m}$  and 1.5 mm, respectively. This indicates that the extent of wear is mitigated in these textured samples compared to the untreated sample (a).





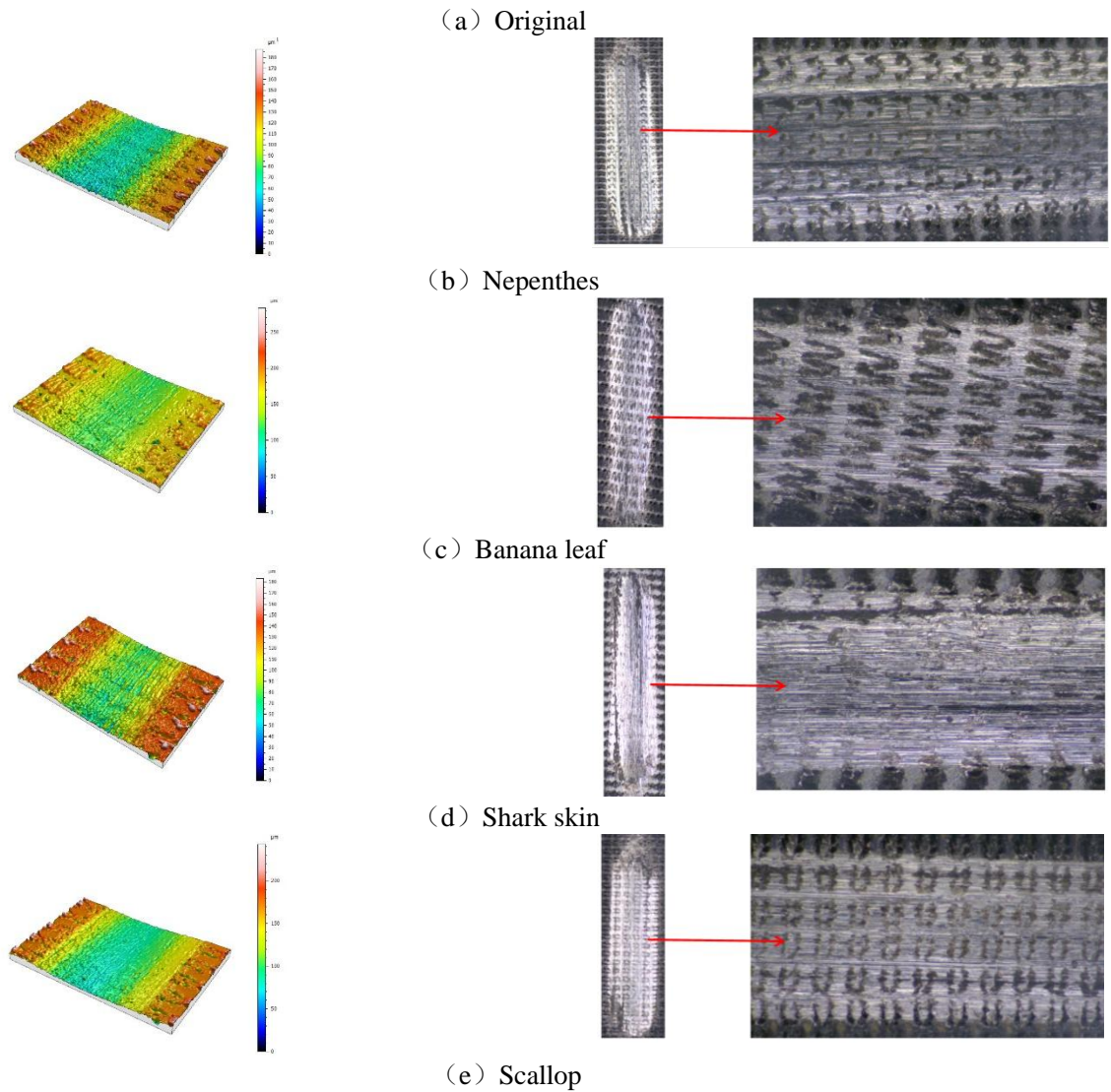


Figure 7. 3D contours and wear marks of TC4 titanium alloy and original film with different weaving patterns

From Figure 7, it is also evident that the surface textures are not completely worn away, indicating that surface texturing can enhance the wear resistance of titanium alloy materials to some extent. Among the textures, the banana leaf texture retains the most residual structure, and its wear scar is the shallowest, suggesting that the banana leaf texture provides the best improvement in wear resistance. The shark skin texture follows in performance, the pitcher plant texture ranks third, and the scallop texture performs the least effectively.

### 3.2 Influence of different dimensions of the same weave pattern on tribological properties of TC4 titanium alloy

#### (1) Analysis of Friction Coefficient Variation

This section examines the variation in the friction coefficient of TC4 titanium alloy samples at room temperature by engraving pitcher plant textures of different sizes (250  $\mu\text{m}$ , 400  $\mu\text{m}$ , and 550  $\mu\text{m}$ ) on their surfaces.

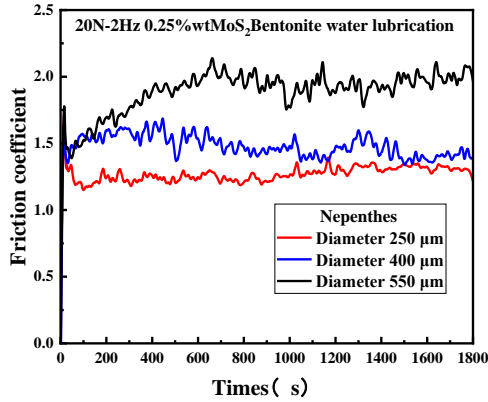


Figure.8 Comparison of real-time friction coefficients of TC4 titanium alloys marked with Nepenthes textures of different sizes

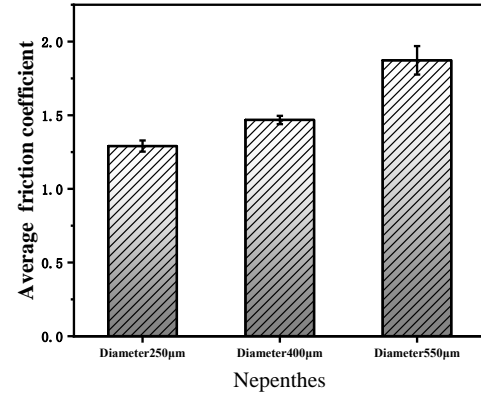


Figure.9 Comparison of average friction coefficients of TC4 titanium alloys marked with Nepenthes textures of different sizes

From Figure 8, it can be observed that the friction coefficient of the TC4 titanium alloy samples changes correspondingly with variations in texture size. Over time, as the friction coefficient stabilizes, the curve for the 250 μm diameter pitcher plant texture lies at the bottom, the 400 μm diameter texture in the middle, and the 550 μm diameter texture at the top. By calculating the average friction coefficient during the stable friction phase after 600 seconds, the following results were obtained: 1.285 for the 250 μm diameter texture, 1.447 for the 400 μm diameter texture, and 1.960 for the 550 μm diameter texture, which is higher than the friction coefficient of the original sample. This indicates that the 250 μm diameter texture provides the best anti-friction performance. As the lateral size of the texture increases, the improvement in the tribological performance of the titanium alloy sample diminishes. Moreover, when the size reaches 550 μm, the texture not only fails to reduce

friction but also exacerbates the wear of the TC4 titanium alloy.

## (2) Analysis of Wear Rate Variation

Figure 14 illustrates the wear rates of pitcher plant textures with different sizes at room temperature. The height of the cylindrical bars in the figure indicates that the wear rate of the 250 μm diameter texture is lower than those of the 400 μm and 550 μm diameter textures. Notably, the wear rate of the 550 μm diameter texture is  $13.1 \times 10^{-4} \text{ mm}^3/(\text{N}\cdot\text{m})$ , which is higher than that of the original sample at  $10.5 \times 10^{-4} \text{ mm}^3/(\text{N}\cdot\text{m})$ . This demonstrates that textures of different sizes have varying effects on improving the wear resistance of titanium alloy materials. The 250 μm diameter texture performs the best, followed by the 400 μm diameter texture. In contrast, the 550 μm diameter texture not only fails to enhance wear resistance but also exacerbates wear.

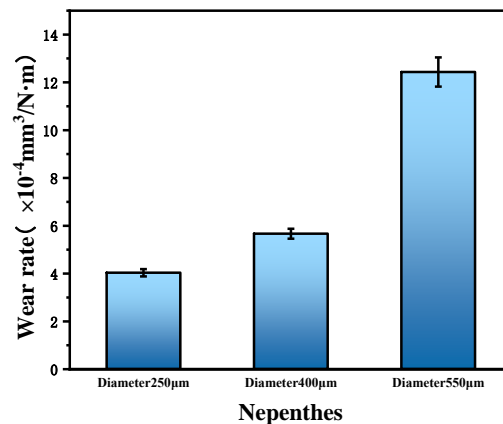


Figure.10 Comparison of wear rates of TC4 titanium alloys marked with Nepenthes textures of different sizes



### (3) Surface Morphology Analysis

Figure 11 below presents the three-dimensional and cross-sectional two-dimensional wear scar profiles of TC4 titanium alloy samples engraved with pitcher plant textures of different sizes. The left side of Figure 11 shows the three-dimensional wear scar color maps for diameters of 250  $\mu\text{m}$ , 400  $\mu\text{m}$ , and 550  $\mu\text{m}$ , while the right side displays the corresponding cross-sectional two-dimensional wear scar profiles at the deepest points of the wear scars. From the figure, it is evident that

Figure 11(a), representing the 250  $\mu\text{m}$  diameter texture, exhibits relatively shallow wear. Based on the cross-sectional two-dimensional wear scar profile, the wear scar depth and width are measured to be 69  $\mu\text{m}$  and 1.4 mm, respectively. In contrast, the wear severity increases for Figure 11(b) 400  $\mu\text{m}$  diameter and (c) 550  $\mu\text{m}$  diameter textures, with wear scar depths and widths of 82  $\mu\text{m}$  and 1.5 mm, and 131  $\mu\text{m}$  and 1.6 mm, respectively.

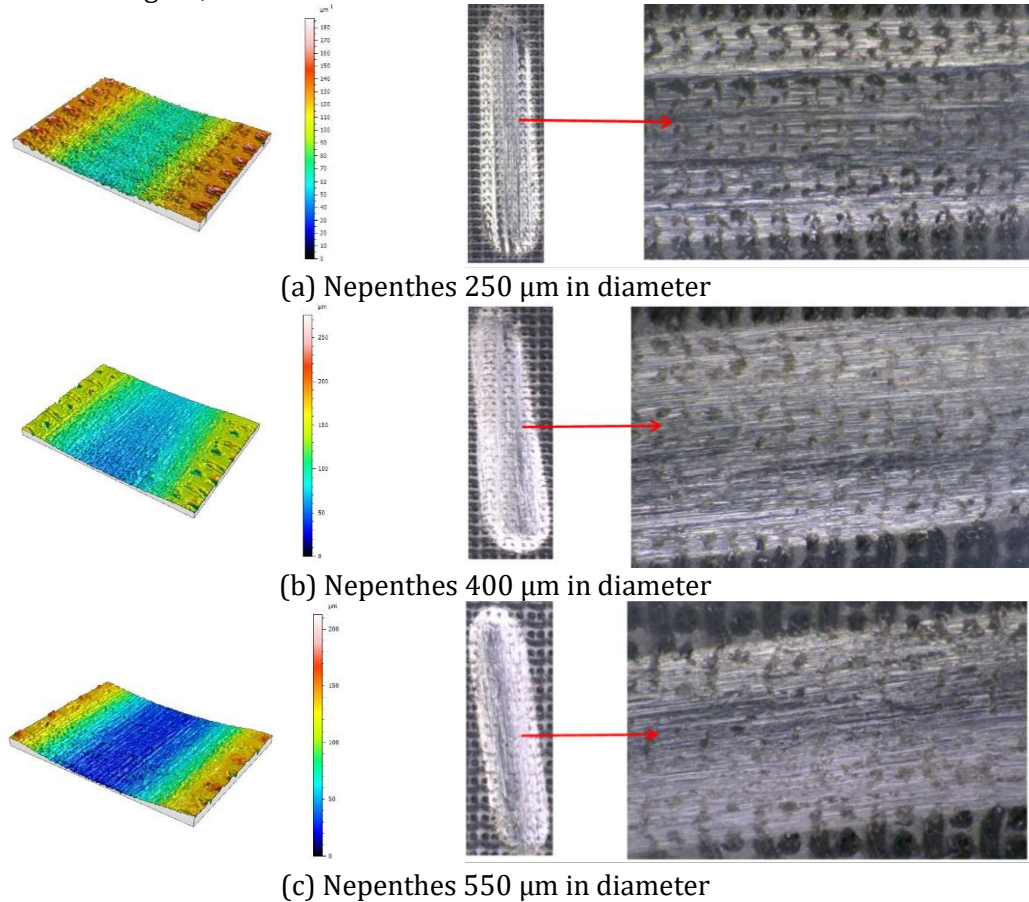


Figure.11 TC4 titanium alloy with Nepenthes textures of different sizes marked with 3D contours and wear marks

From Figure 11, it can be observed that the 250  $\mu\text{m}$  diameter pitcher plant texture, subjected to friction testing under the same experimental conditions, retains its surface texture without being completely worn away. In contrast, the 400  $\mu\text{m}$  and 550  $\mu\text{m}$  diameter pitcher plant textures show relatively shallower residual textures, indicating deeper wear scars. This suggests that the 250  $\mu\text{m}$  diameter texture exhibits better wear resistance compared to the larger-sized textures.

### 3.3 Influence of different densities of the same weave pattern on tribological properties of TC4 titanium alloy

#### (1) Analysis of Friction Coefficient Variation

This section examines the variation in the friction coefficient and wear volume of TC4 titanium alloy samples at room temperature by engraving pitcher plant textures with different area ratios (60%, 70%, and 80%) on their surfaces. From Figure 12, it can be observed that the friction coefficient of the TC4 titanium alloy samples changes correspondingly with variations in texture density. Over time, as the friction coefficient stabilizes, the curve for the 30% area ratio texture lies at the bottom, the 20% area ratio texture in the middle, and the 10% area ratio texture at the top.

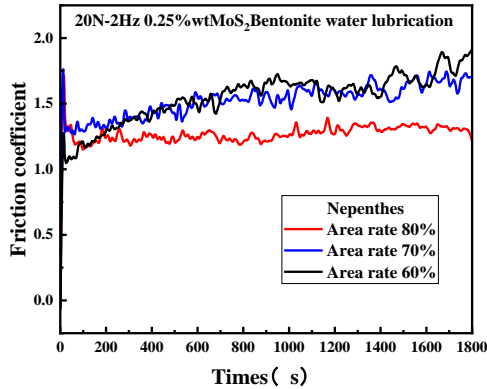


Figure.12 Comparison of real-time friction coefficients of TC4 titanium alloys marked with different density Nepenthes textures

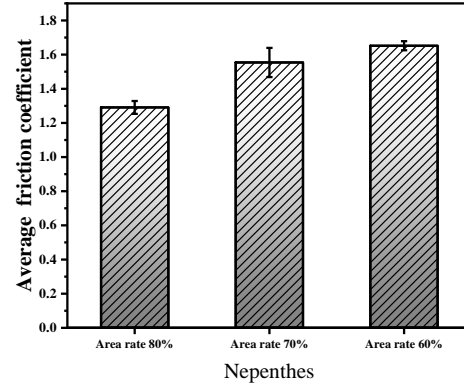


Figure.13 Comparison of average friction coefficients of TC4 titanium alloys marked with different density Nepenthes textures

By calculating the average friction coefficient during the stable friction phase after 600 seconds, the following results were obtained: 1.285 for the 30% area ratio texture, 1.594 for the 20% area ratio texture, and 1.653 for the 10% area ratio texture. This indicates that the 30% area ratio texture provides the best anti-friction performance. As the area ratio decreases, meaning the distance between textures increases, the improvement in the tribological performance of the titanium alloy sample diminishes.

Figure 14 above illustrates the wear rates of pitcher plant textures with different area ratios (60%, 70%, and 80%) at room temperature. The height of the cylindrical bars in the figure indicates that the wear rates of the textures decrease sequentially as the area ratio increases from 60% to 80%. This demonstrates that textures with different densities (area ratios) have varying effects on improving the wear resistance of titanium alloy materials. The 80% area ratio texture performs the best, followed by the 70% area ratio texture, while the 60% area ratio texture exhibits the least improvement.

## (2) Analysis of Wear Rate Variation

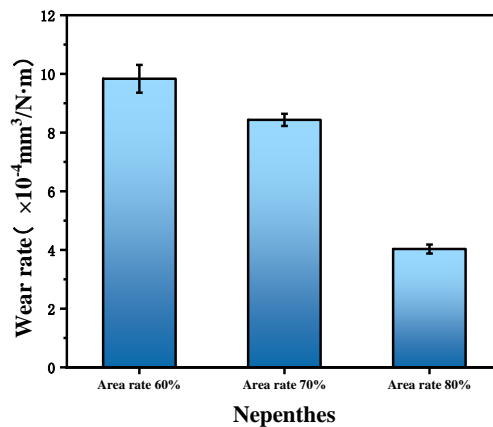


Figure.14 Comparison of wear rates of TC4 titanium alloys marked with different density Nepenthes textures

## (3) Surface Morphology Analysis

Figure 15 presents the three-dimensional wear scar profiles of TC4 titanium alloy samples engraved with pitcher plant textures of different densities (area ratios). From the figure, it is evident that Figure 15(a), representing the 80% area ratio texture, exhibits

relatively shallow wear, with a wear scar depth and width of 69  $\mu\text{m}$  and 1.4 mm, respectively. In contrast, the wear severity increases for Figure 15(b) 70% area ratio and (c) 60% area ratio textures, with wear scar depths and widths of 81  $\mu\text{m}$  and 1.4 mm, and 86  $\mu\text{m}$  and 1.5 mm, respectively.

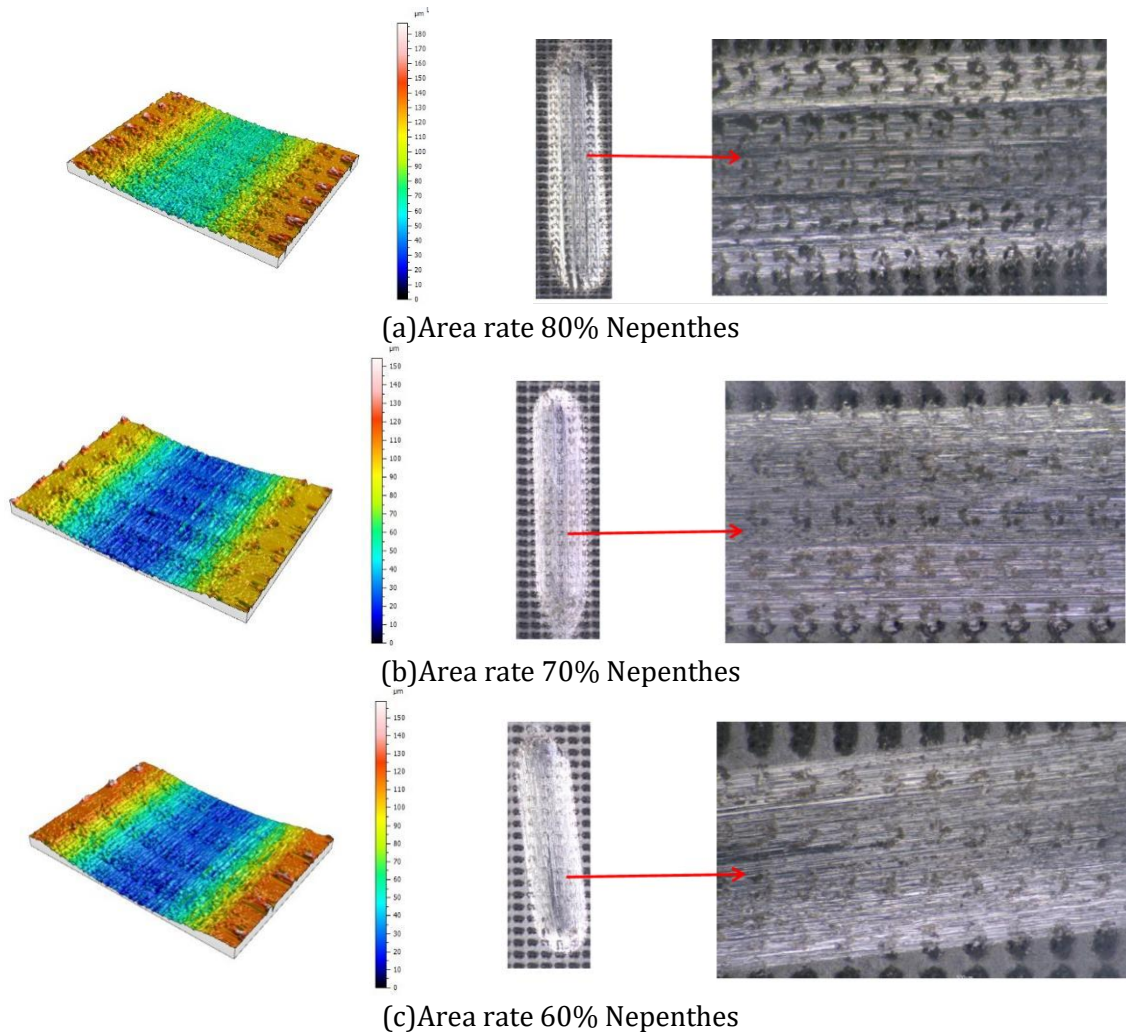


Figure.15 Marked TC4 titanium alloy with different density Nepenthes texture three-dimensional wear contour

From Figure 15, it is also evident that the 80% area ratio pitcher plant texture, when subjected to friction testing under the same experimental conditions, retains its surface texture without being completely worn away. In contrast, the 70% and 60% area ratio textures show relatively shallower residual textures, indicating deeper wear scars. This suggests that the 80% area ratio texture provides better wear resistance compared to the lower area ratio textures.

#### 4. Conclusion

(1) The experimental results demonstrate that surface texturing significantly enhances the anti-friction and wear resistance properties of titanium alloy materials. The influence of different biomimetic texture patterns on anti-friction performance varies notably: the pitcher plant texture exhibits the best anti-friction performance, followed by the scallop texture, the banana

leaf texture, and finally the shark skin texture, which performs the least effectively. In terms of wear resistance improvement, the banana leaf texture shows the most significant enhancement, followed by the shark skin texture, the pitcher plant texture, and the scallop texture, which performs the worst. Comprehensive analysis of both anti-friction and wear resistance properties indicates that the pitcher plant texture provides the most effective improvement in the tribological performance of titanium alloy materials.

(2) Further experiments on the geometric parameters of the pitcher plant texture reveal that changes in texture size and density significantly affect the tribological performance of titanium alloy materials. The 250 μm diameter texture provides the best anti-friction and wear resistance performance. As the lateral size of the texture increases, the improvement in anti-friction and wear resistance diminishes, and when the

size reaches 550  $\mu\text{m}$ , the texture not only fails to reduce friction but also exacerbates wear. Similarly, when the texture density changes, the tribological performance of the titanium alloy material is also affected. The 80% area ratio texture offers the best anti-friction and wear resistance performance. As the area ratio decreases, the improvement in tribological performance weakens, with the 70% area ratio texture performing second best and the 60% area ratio texture showing the least improvement. By designing and investigating different gradients of size and density, it was found that, within a certain parameter range, smaller sizes and larger area ratios result in better improvements in the anti-friction and wear resistance properties of titanium alloy materials.

The research is based on the Natural Science Foundation Project of Sichuan Province (2023NSFSC0871) : Research on the Tribological Properties of Titanium Alloys Modified by Texture-Synergistic Nanoparticles and Sichuan Province College Students' Innovation and Entrepreneurship Training Program Project: Research and Development of Texture-Synergistic Nanoparticle Modified Wear-resistant Titanium Alloy Surface (S202410623045).

## References

- [1] X. H. Lu, Y. Shu, G. X. Zhao, J. F. Xie, and Y. Xue, "Research and Application Progress of Ti Alloy Oil Country Tubular Goods," *Rare Metal Materials and Engineering*, vol. 43, no. 6, pp. 1518-1524, Jun, 2014.
- [2] Q. Li, Q. L. Liu, Y. J. Du, B. Li, Y. J. Wang, and W. W. Xu, "Advances in Optimization Design and Application of Textured Surfaces," *China Surface Engineering*, vol. 34, no. 6, pp. 59-73, Dec, 2021.
- [3] D. B. Hamilton, J. A. Walowit, and C. M. Allen, "A Theory of Lubrication by Microirregularities," *Journal of Basic Engineering*, vol. 88, no. 1, pp. 177-185, 1966.
- [4] N. M. Lin, R. Z. Xie, J. J. Zou, Z. X. Wang, Y. Ma, Z. H. Wang, and B. Tang, "Research Progress on Surface Texture for Improving Tribological Properties of Titanium Alloys," *Rare Metal Materials and Engineering*, vol. 47, no. 8, pp. 2592-2599, Aug, 2018.
- [5] Z. Y. Zhou, D. Q. Chen, C. S. Yuan, Q. W. Dai, W. Huang, and X. L. Wang, "State of Art in Tribological Design and Surface Texturing of Gear Surfaces," *China Surface Engineering*, vol. 37, no. 4, pp. 61-78, Aug, 2024.
- [6] L. X. Li, Y. F. Huang, Z. G. Xing, Z. X. Li, and H. D. Wang, "Research Progress of Ultrafast Laser Fabrication of Biomimetic Textures," *China Surface Engineering*, vol. 36, no. 3, pp. 1-21, Jun, 2023.
- [7] Jie Sun, "Study on Surface wettability of sliding zone of leaf cage of *Nepenthes simulans*," M.S. 2021.
- [8] X. B. Cui, K. Yan, and J. X. Guo, "Bio-inspired fabrication, mechanical characterization and cutting performance evaluation of  $\text{Al}_2\text{O}_3/\text{TiC}$  micro-nano-composite ceramic with varying microscopic surfaces," *Ceramics International*, vol. 45, no. 7, pp. 8286-8299, May, 2019.
- [9] Zhang Jinbo, Tong Jin, and Ma Yunhai, "Abrasive wear characteristics of deep cutting blade on bionic rib structure surface Journal of Jilin University (Engineering and Technology Edition), vol. 45, no. 01, pp. 174-180, 2015.
- [10] Du Hongyi, He Lin, Du Hongxing, Ma Kejing, and Li Yaping, "Bionic tribological tool texture design Modular Machine Tool and Automatic machining Technology," no. 04, pp. 138-142, 2016.
- [11] Z. Wu, Y. Q. Xing, P. Huang, and L. Liu, "Tribological properties of dimple-textured titanium alloys under dry sliding contact," *Surface & Coatings Technology*, vol. 309, pp. 21-28, Jan, 2017.
- [12] B. Zhang, W. Huang, J. Q. Wang, and X. L. Wang, "Comparison of the effects of surface texture on the surfaces of steel and UHMWPE," *Tribology International*, vol. 65, pp. 138-145, Sep, 2013.
- [13] S. Costil, A. Lamraoui, C. Langlade, O. Heintz, and R. Oltra, "Surface modifications induced by pulsed-laser texturing-Influence of laser impact on the surface properties," *Applied Surface Science*, vol. 288, pp. 542-549, Jan, 2014.
- [14] D. Choudhury, T. Roy, I. Krupka, M. Hartl, and R. Mootanah, "Tribological investigation of ultra-high molecular weight polyethylene against advanced ceramic surfaces in total hip joint replacement," *Proceedings of the Institution of Mechanical Engineers Part J-Journal of Engineering Tribology*, vol. 229, no. 4, pp. 410-419, Apr, 2015.
- [15] M. Wakuda, Y. Yamauchi, S. Kanzaki, and Y. Yasuda, "Effect of surface texturing on friction reduction between ceramic and steel materials under lubricated sliding contact," *Wear*, vol. 254, no. 3-4, pp. 356-363, Feb, 2003.
- [16] P. L. Menezes, and S. V. Kailas, "Role of surface texture and roughness parameters on friction and transfer film formation when UHMWPE sliding against steel," *Biosurface and Biotribology*, vol. 2, no. 1, pp. 1-10, 2016/03/01/, 2016.